Radiological Physics and Technology (2019) 12:86–95
https://doi.org/10.1007/s12194-018-00495-2

Performance evaluation of the CyberKnife system in real-time target tracking during beam delivery using a moving phantom coupled with two-dimensional detector array

Bin Yang[1] · Tin Lok Chiu[1] · Wai Kong Law[1] · Hui Geng[1] · Wai Wang Lam[1] · Tat Ming Leung[2] · Lok Hang Yiu[2] · Kin Yin Cheung[1] · Siu Ki Yu[1]

Received: 13 April 2018 / Revised: 16 December 2018 / Accepted: 19 December 2018 / Published online: 2 January 2019

Abstract
The aim of the current study was to evaluate the tracking error of the Synchrony Respiratory Tracking system by conducting beam-by-beam analyses to determine the variation in the tracking beams measured during target motion. A moving phantom of in-house design coupled with a two-dimensional (2D) detector array was used to simulate respiratory motion in the superoinferior (SI) and anteroposterior (AP) direction. A styrofoam block with four implanted fiducial markers was placed on top of the detector to enable the fiducial-based respiratory tracking. Measurements were performed with the phantom under either stationary mode or sinusoidal motion of 6-s cycle and 15/20-mm amplitude at SI and AP direction. The measurement data were saved as movie files that were used to calculate the center shift of the beam with 100-ms sampling time. The tracking accuracy of the system was defined as the targeting error, which could be tracked with probability of $>95\%$ (Ep95). The mean $\pm$ standard deviation of Ep95 was 0.28 ± 0.08 mm under stationary condition; 0.66 ± 0.23 mm (range: 0.28–1.22 mm) under sinusoidal respiratory motion. The maximum drift of the beam center for all beam paths was 2.7 mm. The tracking accuracy of CyberKnife Synchrony system was successfully evaluated using a moving phantom and 2D detector array; the maximum tracking error was <1.5 mm for sinusoidal motion of amplitude ≤ 20 mm.

Keywords CyberKnife · Synchrony · Target-tracking accuracy · 2D detector array

1 Introduction

Advancements in image-guided radiotherapy and motion management have resulted in the routine implementation of hypofractionated stereotactic body radiation therapy (SBRT) in clinical settings [1–3]. CyberKnife (Accuray Inc., Sunnyvale, CA, USA), which is capable of real-time target tracking, allows for noninvasive stereotactic radiosurgery (SRS) and SBRT by delivering high-dose radiation precisely to the tumor volume in the body [3–5]. CyberKnife is capable of continually detecting, tracking, and correcting tumor motion due to movement of the patient during the treatment delivery [6–9]. This unique feature is realized by two target-tracking methods: fiducial tracking combined with the Synchrony system and Xsight Lung Tracking (XLT); fiducial tracking requires the fiducial markers to be implanted near or inside the tumor, whereas XLT relies on the difference in the soft-tissue contrast. Both methods can be combined with the Synchrony Respiratory Tracking System to synchronize beam targeting with the tumor motion caused by the patients' respiratory motion.

Unlike the conventional LINAC-based system, CyberKnife has unique features of both tracking methods and hardware design. Therefore, the geometric and dosimetric accuracy of real-time target tracking and utilization of robotics during treatment delivery must be appropriately evaluated and validated. Several studies to evaluate the accuracy of real-time target tracking were previously conducted [8–11]. The overall targeting accuracy is defined as the offset between the centroid of the delivered 70% isodose line in a sphere and known centroid position of the planned dose

✉ Bin Yang
Kimi.B.Yang@hksh.com

[1] Medical Physics and Research Department, Hong Kong Sanatorium & Hospital, 2 Village Road, Happy Valley, Hong Kong, China

[2] Biomedical Engineering Department, Hong Kong Sanatorium & Hospital, 2 Village Road, Happy Valley, Hong Kong, China

distributions. The AAPM Task Group 135 suggests a tolerance of 1.5 mm for motion-tracking treatments involving Synchrony [12]; however, a tighter tolerance of 0.95 mm for isocentric end-to-end (E2E) tests can be achieved for both fiducial-based Synchrony and XLT. Many studies investigated the tracking accuracy of either XLT or fiducial-based Synchrony using phantom study and clinical data [13–16]. In addition, some studies focused on the tracking errors of each beam using a charge-coupled device camera fixed onto the head of the LINAC [17] or webcam, and calibrated grid mounted on a moving phantom [18]; however, those studies focused on visually tracking an external surrogate such as a moving ball or laser point and did not measure the radiation beam that contributed to the final target-tracking accuracy. A recent study reported the accuracy of the Sychrony system using a plastic scintillator, which derived the beam position from the scintillation light after application of quantitative methods to correct the effective center inside the 1-cm scintillator [19]. Therefore, possible variation in the radiation beam during target tracking in individual treatment beam needs to be determined, which may be one of many causes of the overall tracking error.

According to AAPM Task Group 135, full set of beam-path calibration (both 1st Order and 2nd Order) has been defined specifically and is performed by Accuray's installation or service personnel using the isopost [12]. Although the general Synchrony system consists of many components, the aim of the present study was to perform a more basic evaluation of its tracking accuracy without considering the absolute beam-path accuracy from the path calibration. We developed a moving phantom to simulate respiratory motion, and mounted a two-dimensional (2D) detector array on the phantom to measure the radiation field directly. By utilizing the time-resolved function of our system, we could directly measure the target-tracking accuracy for each beam.

2 Materials and methods

All experiments were conducted using the CyberKnife M6 system, comprising a 6-MV linear accelerator mounted on a robotic arm. The target locating system (TLS) includes two ceiling-mounted orthogonal diagnostic X-ray sources paired with flat-panel detectors under the floor to acquire orthogonal live digital radiographic images of the internal targets, bony structures, or fiducial markers inside the patient. The Synchrony Respiratory Tracking System has capability to track the respiratory motion of a tumor in real time by continuously monitoring three light-emitting diode (LED) markers attached to the patient using a camera array mounted on the ceiling. In this study, the fiducial-based Synchrony tracking method was selected.

2.1 Phantom configuration

A moving phantom of in-house design, which was previously used for the commissioning of the gated VMAT [20], was modified to work with the 2D detector array, Octavius Detector 1500 (PTW-Freiburg, Freiburg, Germany) (Fig. 1). A styrofoam block was implanted with four fiducial markers (Beekley Corporation, Bristol, CT, USA) to enable the fiducial-based Synchrony Respiratory Tracking System and firmly fixed on the surface of the 2D array. The moving phantom was capable of moving in both *Z* and *Y* directions

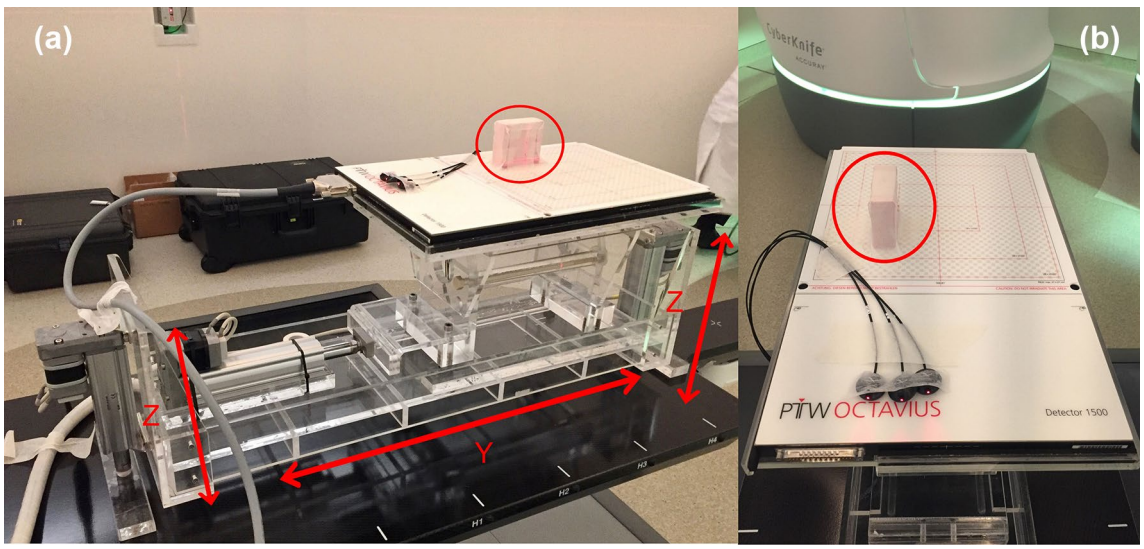

Fig. 1 In-house-designed moving phantom coupled with a 2D detector array. Three LED markers were fixed to the surface of the detector array. Red arrows indicate the *Z* and *Y* directions of motion and red circles indicate the location of the styrofoam block with implanted fiducials

independently, where the left–right, superoinferior (SI), and anteroposterior (AP) directions were defined as *X, Y*, and *Z*, respectively. In this study, for the phantom's motion, two different sinusoidal waves with peak-to-peak amplitudes of 15 and 20 mm were applied in the *Y* and *Z* directions with a phase shift of 0° and fixed period of 6 s.

A 2D detector array with a total of 1405 vented ionization chambers of size of 4.4 mm × 4.4 mm × 3 mm, was used in this study (Fig. 1b). The detector array was placed on a custom-made polymethyl methacrylate holder that was firmly installed on the moving phantom. The interleaving arrangement of the ionization chambers allowed the measurement of profiles with a spatial resolution of 5 mm.

By utilizing the specific software provided with the Octavius 4D phantom (PTW-Freiburg, Freiburg, Germany), the measured data were saved as movie files (.xcc) with a sampling time of 100 ms, which could record more than 80 frames for each beam and enabled frame-by-frame analysis of the beam-center shift. The position of the beam center on each frame was defined as the centroid of the *X* and *Y* profiles based on 70% of its maximum intensity. Most measured beams were at an oblique angle to the 2D detector array, which caused skewness of the radiation field; hence, the calculated beam centers in this study did not represent the actual radiation center.

In addition, film measurements were conducted under different modes of motion and compared with the results of 2D array. Gafchromic EBT^3 film (Ashland Inc., Covington, KY, USA) was placed at 7.5-mm depth in solid water slabs, considered as the effective measurement point of the ionization chamber inside the 2D array. The same styrofoam block was placed on top of the solid water slab to enable real-time tracking. A 48-bit color scanner, Epson Expression 10000XL (Epson, Suwa, Nagano, Japan), was used to scan the film without color correction and a pre-determined calibration curve was applied to convert the pixel value to dose. To avoid saturation of the measured dose, the original quality assurance (QA) plan was scaled down to ensure maximum dose at the film position of around 7.2 Gy.

2.2 CyberKnife QA plan

Planning computed tomography (CT) images of the moving phantom were acquired using a CT simulator (Siemens AG, Munich, Germany) with parameters of 120 kVp, 400 mAs, and 1-mm slice thickness. Figure 2a–d present CT images of the system and Fig. 2e, f present orthogonal-kV X-ray images acquired during the treatment setup, which demonstrate that the markers can be successfully located. An isocentric plan involving a short-body path with a total of 31 beams was created with a fixed 60-mm cone (Fig. 2g), and 150 MU was also fixed for all beams to ensure that the beam-on time for any beam was larger than one respiratory cycle of the moving phantom. The isocenter was arbitrarily selected with localization at the center of an ion chamber at 5-cm distance from the styrofoam block, because we did not aim to measure the accuracy of the absolute beam path. The contoured styrofoam block was intentionally avoided in MultiPlan, the treatment planning system of the CyberKnife, to reduce uncertainty in the measurements. The setup of the phantom under implementation of the QA plan is shown in Fig. 2h.

To determine the difference between Synchrony and conventional fiducial tracking technique of CyberKnife, the QA plan was delivered with the phantom set in motion and at stationary mode separately. For each setting of the phantom

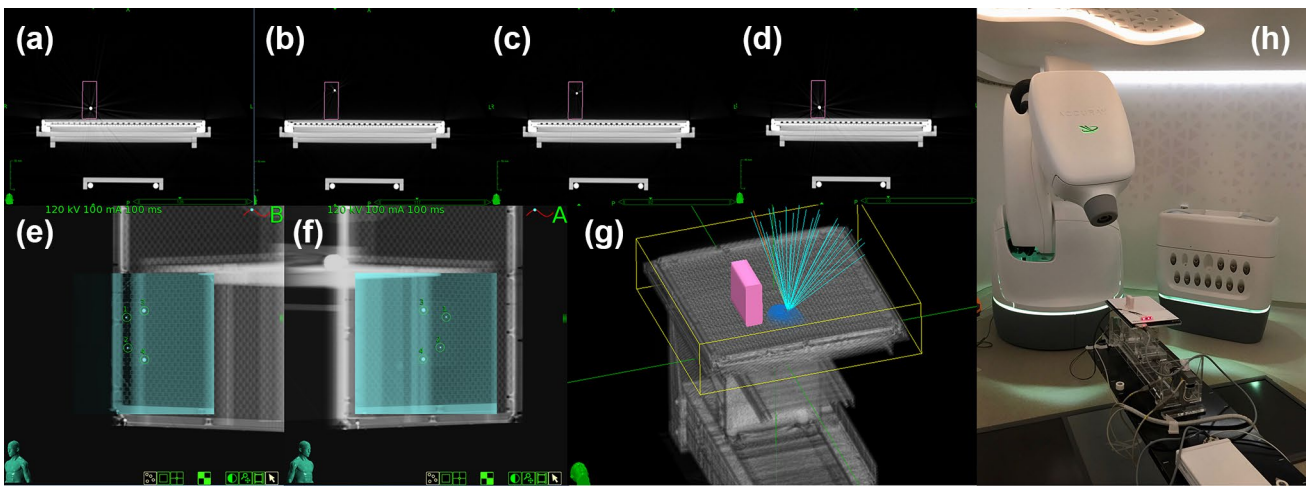

Fig. 2 **a–d** Scanned CT images of the verification system showing the location of the four fiducials implanted in the styrofoam block. **e, f** Orthogonal-kV X-ray images acquired at the console computer. **g** 3D view of the beam paths in MultiPlan, treatment planning system of the CyberKnife. **h** The system setup during delivery of the treatment plan

with different moving amplitude, 10 repeated measurements were obtained.

2.3 Analysis for correlation and prediction model errors

The Synchrony Respiratory Tracking System is based on a correlation model between the position of the external LED marker and internal target [6, 21]. The correlation model estimates the target position which is sent to the robotic manipulator directly. However, there is a time delay caused by communication latencies between the robotic manipulator and LINAC inertia. The system then constructs a prediction model based on the LED-marker location to calculate the future position of the target to compensate for the mechanical time delay [6, 21]. The log files generated by Synchrony were extracted after each treatment delivery. The prediction model error was calculated by comparing the predicted position of the robotic manipulator with its actual position after a time delay and stored in the log file, *Predictor.log*. The correlation error, which was recorded in the log file, *ModelPoint.log*, was defined as the difference between the location of tumor as determined by the two orthogonal X-ray images and that calculated by the latest correlation model [6, 22, 23]. For each treatment delivery, the extracted *ModelPoint.log* contained more than 100 samples that represented the captured X-ray images, while the *Predictor.log* contained more than 21,000 samples.

2.4 Precision of detected beam-center shift using 2D detector array

To assess the precision of the detected beam-center shift using our proposed method, the center shifts measured by the 2D detector array were compared with those of the actual robot that were intentionally introduced with a range of 0 to 3 mm. Because there were 31 beams at different robot positions, we manually introduced two beams with incident angle of 0° and 40° relative to the plane of the detector array. For the beam with incident angle of 0°, position shifts were manually introduced in the *X, Y*, and diagonal directions, and the final calculated results were averaged. The beam with incident angle of 40° was tilted in the *Y* direction. Robot shifts were then separately introduced in the *X, Y*, and diagonal directions.

2.5 Tracking accuracy of CyberKnife

A previously described evaluation method [17] was used in this study, and the beam center was analyzed and recorded frame-by-frame. The targeting error for each beam path, which could be tracked with probability of > 95%, was calculated as follows:

$$\text{targeting error (Ep95)} = \text{mean} + 1.96 \times \text{SD},$$

where the mean and SD are the average and standard deviation of the calculated distance between the beam centers and their centroid, respectively. The accuracy of CyberKnife was defined as the median value of Ep95 for all 31 beam paths involved in this study, i.e., Ep95med.

2.6 Statistical analyses

The Ep95 was calculated for each beam after each delivery. Student's *t* test was used to compare different motion settings of the phantom and the differences were considered statistically significant at the 95% confidence level ($P < 0.05$). Linear regression was also performed to fit the model to the data of Ep95 and incident angle of the beam. The final tracking error was calculated as the overall mean ± SD for all beams.

3 Results

3.1 Correlation and prediction model errors

Table 1 presents a summary of the overall correlation and prediction model errors. We expected similar values for the prediction error at *Y* and *Z*, because the same motion amplitude was used in both directions. Furthermore, the prediction errors at *Y* and *Z* were significantly larger than that at *X* (all $P < 0.0001$), because there was no movement of the phantom in the *X* direction in our experiments. There was no statistically significant difference in the correlation error for the motion amplitude at all three directions (all $P > 0.25$), and

Table 1 Overall correlation and prediction model errors calculated by the target locating system

Motion amplitude (mm)	Direction	Mean ± SD (mm)	Range (mm)
Correlation error			
15	*X*	0.10 ± 0.06	− 0.23–0.21
	Y	0.11 ± 0.09	− 0.37–0.31
	Z	0.12 ± 0.09	− 0.45–0.27
20	*X*	0.10 ± 0.08	− 0.38–0.29
	Y	0.13 ± 0.10	− 0.40–0.37
	Z	0.13 ± 0.10	− 0.44–0.48
Prediction error			
15	*X*	0.001 ± 0.003	0.00–0.03
	Y	0.10 ± 0.02	0.05–0.16
	Z	0.10 ± 0.02	0.06–0.17
20	*X*	0.001 ± 0.001	0.00–0.01
	Y	0.16 ± 0.03	0.06–0.25
	Z	0.16 ± 0.03	0.07–0.24

the prediction error for larger motion amplitudes had slightly larger mean value at Y and Z (all $P < 0.0001$).

3.2 Integrated dose

Similar to the conventional film measurement, the integrated dose was easily measured using our phantom. A representative case of the final 2D dose distribution at completion of treatment delivery is shown in Fig. 3a. The maps of the dose difference between the 1-d benchmark and that at different days with the same or different motion amplitude are shown in Fig. 3b–d. The dose maps at different days were very similar, with maximum deviation of the peak dose of $< 0.2\%$. After the original data were properly interpolated, the conventional gamma passing rate was $> 99\%$ under criteria of 1-mm distance to agreement, 2% dose difference, and 10% threshold. Dose differences occurred mainly in the low-dose region that was out of the 10% isodose line. The largest deviation in the low-dose region was $< 3\%$ of the peak dose and originated from the differences between the phantom in motion and at stationary mode. The X and Y profiles (Fig. 4a, b) further indicated that CyberKnife had high accuracy in terms of the dose delivery and the measurements at different days with different motion settings showed good agreement in the high-dose region. The center shifts for all profiles measured by the 2D array were within 0.1 mm.

A representative case of the dose distribution through film measurements at stationary mode of the phantom is shown in Fig. 4c. The normalized dose profiles in crossline direction for both the 2D array and film measurements are

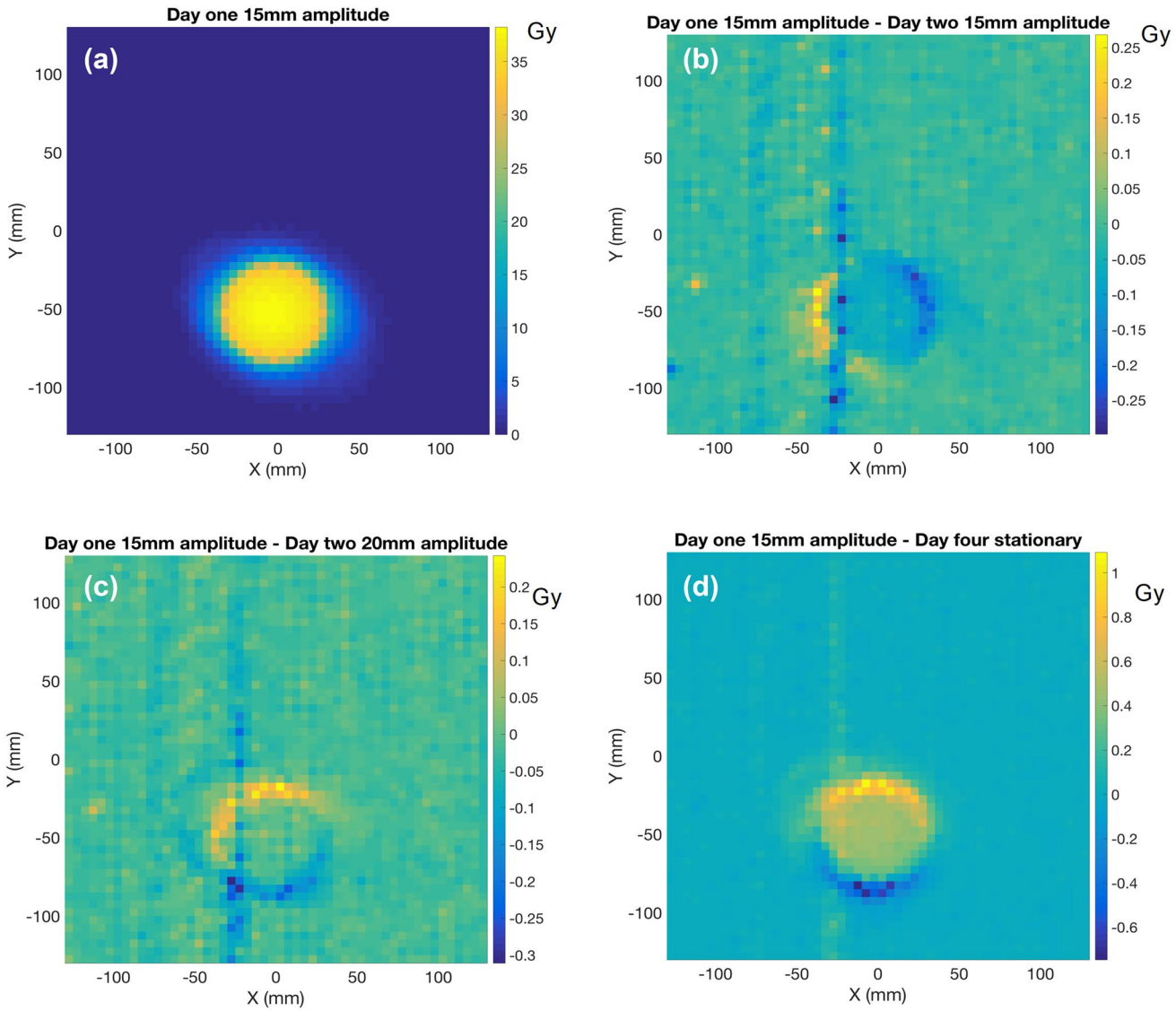

Fig. 3 **a** 2D dose distribution measured for the phantom in motion with 15-mm amplitude on day 1. **b–d** Maps of the difference in dose between the 1-d benchmark and that of different days at the same or different motion amplitude

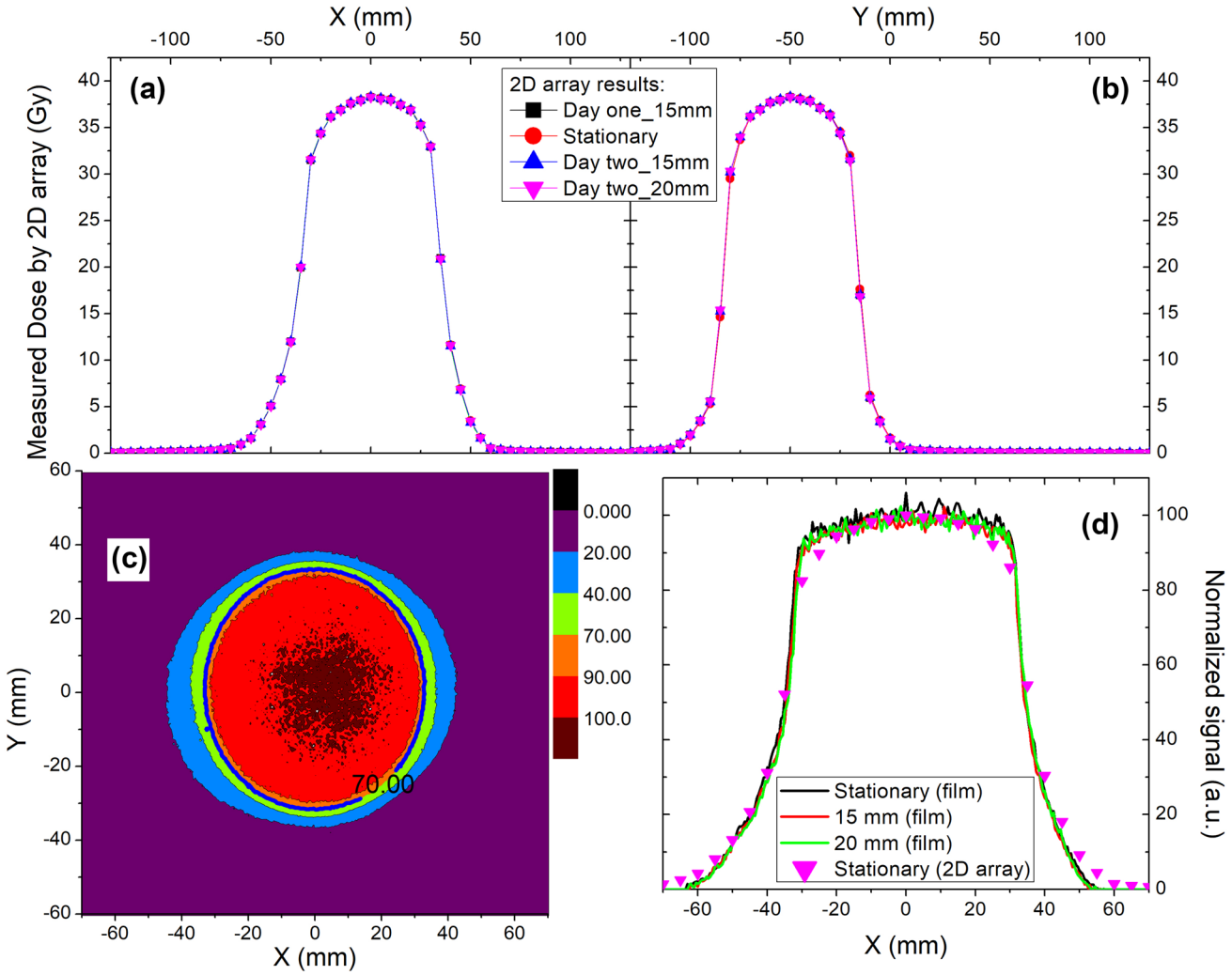

Fig. 4 Integrated dose profiles measured at **a** *X* and **b** *Y* on different days with the same or different motion amplitude. **c** Measured isodose plot using film for the stationary mode. Blue solid line indicates the 70% isodose line. **d** Normalized crossline dose profiles for measurements through both film and 2D array

also plotted (Fig. 4d) for purpose of comparison. Similar to the results of 2D array (Fig. 4a, b), the profiles for different modes of motion were comparable. The differences between the results through film measurement and 2D array at the shoulder and tail region are due to the volume-averaging effect of the relatively large size of the ionization chamber. The calculated center shift through film measurements of <0.26 mm was slightly larger than that through 2D array of <0.1 mm, which may be due to the high level of noise in the film measurements, which had approximately 5% variation at the peak region.

3.3 Targeting accuracy at the stationary mode

Representative frames acquired through the 2D detector array at 100-ms interval for beam paths No. 12 and 31 in the stationary phantom are shown in Fig. 5c, d. Path No. 12 had a more oblique incident angle relative to the detector array. With a sampling time of 100 ms, the signal-to-noise (SNR) ratio of the measured profile was >500 and maximum measured dose for each frame was approximately 10 mGy, which exceeded the lowest dose-range of 0.1 mGy for the 2D detector array. The scatter plots of the beam center for each frame with two complete beam deliveries are shown in Fig. 5a, b.

The mean $\pm$ SD of Ep95 for all beam paths is plotted in Fig. 6. The Ep95med for the stationary phantom was 0.26 mm and mean $\pm$ SD of Ep95 was 0.28 ± 0.08 mm. To clarify the result, we calculated the centroid of the scatter points shown in Fig. 5a, b as the center point of the circle and calculated the percentage of points within the circle. The mean and minimum percentages for all 31 beam paths as a function of the radius of the circle are presented in Table 2.

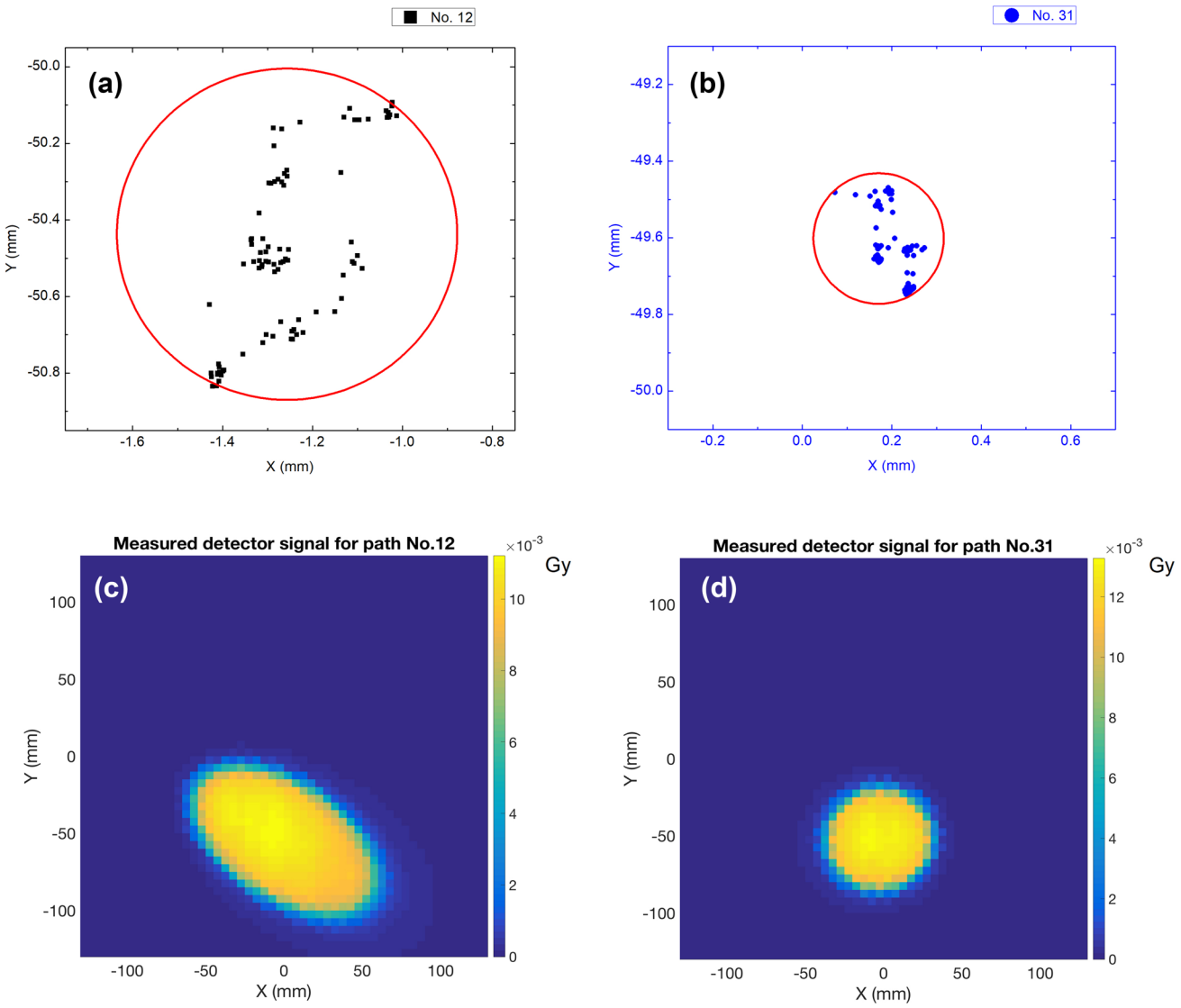

Fig. 5 **a, b** Scatter plots of the beam center calculated from each frame for beam paths Nos. 12 and 31. **c, d** Representative frames measured by the 2D detector array for beam paths Nos. 12 and 31

A circle with radius of 0.3 mm contained > 95% of the beam centers.

The red circles in Fig. 5a, b indicate the maximum drift of the beam center in terms of the maximum distance between scatter points; the maximum drift for all paths is < 0.8 mm.

3.4 Targeting accuracy at sinusoidal motion

The phantom with moving amplitude of 15 and 20 mm showed significantly larger value of the mean ± SD of Ep95 (P values < 0.001 for all beams) as compared to that of the stationary phantom (Fig. 6), and there was no statistically significant difference between the Ep95 values at the two amplitudes ($P > 0.8$ for all beams). The final Ep95 calculated as the average value at the two amplitudes was 0.66 ± 0.23 mm. The maximum and minimum Ep95 of all beam paths was 1.22 and 0.28 mm, respectively, and Ep95med for the phantom in sinusoidal motion was 0.67 mm, which was below the tolerance limit of end-to-end tests performed with Synchrony [21]. The maximum drift of the beam center for beam No. 12 was 2.7 mm for the phantom in motion. The percentage of beam centers within the circle for all beam paths as a function of changing radius is shown in Table 3. A circle with radius of 0.3 mm encompassed only 60.9% of all beam centers and reached a minimum percentage of 19.4% at beam No. 12, which was in contrast to the result for the phantom at stationary mode.

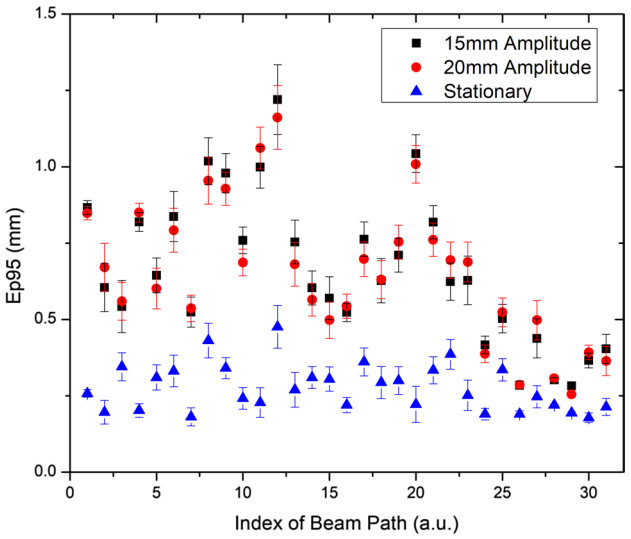

Fig. 6 Calculated Ep95 (and SD) for all beam paths under stationary and moving conditions

Table 2 Mean and minimum percentage for all 31 beam paths as a function of the circle's radius in the stationary phantom

Radius (mm)	Mean (%)	Min (%)
0.5	100	100
0.4	99.6	90.9
0.3	95.6	67.1
0.2	77.0	29.9
0.1	34.3	1.1

Table 3 Mean and minimum percentage for all 31 beam paths as a function of the circle's radius for the phantom in sinusoidal motion

Radius (mm)	Mean (%)	Min (%)
0.95	98.7	91.7
0.8	96.9	81.2
0.7	94.8	70.6
0.6	91.2	60.3
0.5	85.1	46.5
0.4	75.4	33.1
0.3	60.9	19.4

3.5 Precision of the detected shift of the beam center using 2D detector array

For the induced robot shifts of > 0.8 mm, the center shifts for both beams were overestimated, while those for the induced robot shifts of < 0.5 mm were underestimated (Fig. 7a). The overestimation for the beam at 0° was larger than that for the beam at 40° and the maximum deviation was close to 1 mm. Moreover, the measured curve with shifts in the *X* direction for the beam at 40° was very similar to that for the beam at 0°, and the curve with shifts in the diagonal direction was in between the two plotted curves (data not shown in Fig. 7a). In this study, more than 80% of the beam paths had an incident angle of < 40°, hence, the Ep95med probably indicated a robot tracking accuracy better than 0.67 mm.

4 Discussion

The Ep95 value differed by the beam path (Fig. 6), but the pattern and trend of the different beam paths for the phantom in motion were similar to those for the phantom at stationary mode. To determine the angular dependence, the Ep95 values for the different beam paths were plotted as a function of the incident angle (Fig. 7b). Linear regression analysis indicated that the Ep95 was moderately correlated with the incident angle (Pearson correlation coefficient, $r = 0.367$ and adjusted $R^2 = 0.105$; $P = 0.042$), which is in contrast to the result of Sumida et al. [18] of increased tracking error with decreases in the incident angle.

Our study has some limitations. First, the tracking error at *Z* could not be evaluated directly due to the application of 2D array detector; however, it could still be inferred by our results, because the robot shift at *Z* could also cause drift of the beam center in the *X*–*Y* plane. Therefore, the final tracking error was actually a combination of the errors at all three directions. Second, the 2D array detector had limited spatial resolution. In a previous study [23], we introduced a QA method to evaluate the position accuracy of the multileaf collimator at sub-millimeter range by utilizing the finite-sized ion chambers of the same 2D array detector used in the present study. We also determined the correlation between the measured shift and induced robot shift (Fig. 7a); hence, it was possible to achieve sub-millimeter accuracy to detect the drift of the beam center. Third, the correlations between the moving amplitude, cycle of motion, and tracking accuracy were not systematically studied, because our goal was to present a new method to evaluate the tracking accuracy based on the radiation field directly and we mainly focused on the stability of the manipulator system and delivery of the radiation beam. In addition, uncertainty of the Synchrony model also contributes to the final tracking accuracy. Therefore, the tracking error of Synchrony was evaluated with small prediction and correlation model errors in this study, which was realized by selecting the relatively long breathing cycle of 6 s. Moreover, the mechanical performance of the moving phantom with irregular respiratory pattern may affect the results. In particular, Sumida et al. reported that the magnitude of tracking errors was positively correlated with the amplitude of motion and

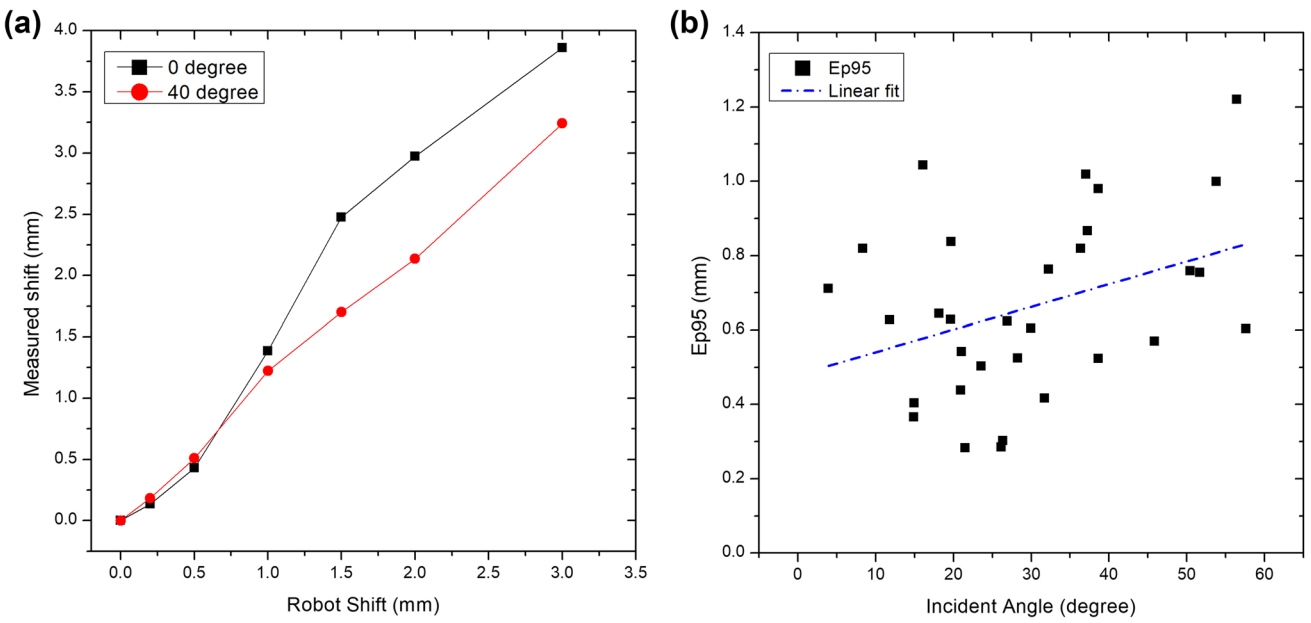

Fig. 7 **a** Correlation curves of the measured shift versus the induced robot shift at incident angle of 0° (averaged from X, Y, and diagonal directions) and 40° (Y direction only). **b** Plot of the Ep95 as a function of incident angle

negatively correlated with the cycle of the sinusoidal motion. The aim of the current study was to determine the effectiveness of the 2D detector array as a convenient tool to evaluate the tracking accuracy of CyberKnife under sinusoidal motion. The proposed technique can be generalized to the tracking errors for irregular respiratory. With regard to the Ep95med of 0.26 mm at the stationary mode, the tracking error should derive from the stability of the radiation field and 2D detector array. The reproducibility of the 2D detector array is supposedly better than 0.5%, which induces a center shift of <0.05 mm; hence, the tracking error at the stationary mode (with Synchrony disabled) was caused mainly by the radiation field itself. Unlike the results presented in **3.1** and those studies [17–19] that combined the accuracy of Synchrony tracking and beam path, the beam-by-beam analysis of the tracking error in **3.3** and **3.4** might not indicate the coincidence between the planned center and actual beam-delivered points correctly. This may be, because the centroid of 70% intensity of the measured profile using 2D array detector does not represent the actual radiation-beam center when the skewness of profiles from the oblique beams are not corrected. Although this is another limitation of our study, as long as a complete beam profile could be collected, the location of plan center would not be a major concern. Therefore, the tracking error was an evaluation of the residual uncertainty of models (although very small), the stability of radiation beam and the mechanical performance of the manipulator system, which includes the vibration of robotic arm, the response to motion model and repeatability of robot. When the coincidence between the planned center and actual beam paths is considered correctly, the final tracking error may be larger than the presented value of Ep95med.

5 Conclusion

We developed a beam-by-beam verification system based on a custom-made moving phantom coupled with a 2D detector array to evaluate the tracking accuracy of the CyberKnife Synchrony system. The drift of the beam center was calculated directly from the radiation field, and the evaluated tracking error ranged from 0.28 to 1.22 mm.

Compliance with ethical standards

Conflict of interest The authors have no relevant conflicts of interest to disclose.

Statement of human and animal rights This study included no animals or humans.

Informed consent Informed consent was not necessary, because no human subjects were involved in this work.

References

1. Solda F, Lodge M, Ashley S, et al. Stereotactic radiotherapy (SABR) for the treatment of primary non-small cell lung cancer:

systematic review and comparison with a surgical cohort. Radiother Oncol. 2013;109:1–7.
2. Ryu SI, Chang SD, Kim DH, et al. Image-guided hypo-fractionated stereotactic radiosurgery to spinal lesions. Neurosurg. 2001;49(4):838–46.
3. Gerszten PC, Ozhasoglu C, Burton SA, et al. CyberKnife frameless stereotactic radiosurgery for spinal lesions: clinical experience in 125 cases. Neurosurg. 2004;55(1):89–98.
4. Van der Voort. van Zyp NC, Prevost JB, Hoogeman MS, et al. Stereotactic radiotherapy with real-time tumor tracking for non-small cell lung cancer: clinical outcome. Radiother Oncol. 2009;91(3):296–300.
5. Unger K, Ju A, Oermann E, et al. CyberKnife for hilar lung tumors: report of clinical response and toxicity. J Hematol Oncol. 2010;3:39.
6. Pepin EW, Wu H, Zhang Y, et al. Correlation and prediction uncertainties in the cyberknife synchrony respiratory tracking system. Med Phys. 2011;38:4036–44.
7. Winter JD, Wong R, Swaminath A, et al. Accuracy of robotic radiosurgical liver treatment throughout the respiratory cycle. Int J Radiat Oncol Biol Phys. 2015;93:916–24.
8. Ho AK, Fu D, Cotrutz C, et al. A study of the accuracy of cyberknife spinal radiosurgery using skeletal structure tracking. Neurosurg. 2007;60(2 Suppl 1):ONS147–156.
9. Yu C, Main W, Taylor D, Kuduvalli G, Apuzzo ML, Alder JR Jr. An anthropomorphic phantom study of the accuracy of Cyberknife spinal radiosurgery. Neurosurg. 2004;55(5):1138–49.
10. Murphy MJ, Cox RS. The accuracy of dose localization for an image-guided frameless radiosurgery system. Med Phys. 1996;23(12):2043–49.
11. Shiomi H, Inoue T, Nakamura S. Quality assurance for an image-guided frameless radiosurgery system using radiochromic film. Radiat Med. 2000;18(2):107–13.
12. Dieterich S, Cavedon C, Chuang CF, Cohen AB, Garrett JA, Lee CL, Lowenstein JR, d'Souza MF, Taylor DD Jr, Wu X, Yu C. Report of AAPM TG 135: quality assurance for robotic radiosurgery. Med Phys. 2011;38(6):2914–36.
13. Seppenwoolde Y, Berbeco RI, Nishioka S, Shirato H, Heijmen B. Accuracy of tumor motion compensation algorithm from a robotic respiratory tracking system: a simulation study. Med Phys. 2007;34(7):2774–84.
14. Hoogeman M, Prevost JB, Nuyttens J, Poll J, Levendaq P, Heijmen B. Clinical accuracy of the respiratory tumor tracking system of the cyberknife: assessment by analysis of log files. Int J Radiat Oncol Biol Phys. 2009;74(1):297–303.
15. Nioutsikou E, Seppenwoolde Y, Symonds-Tayler JR, Heijmen B, Evans P, Webb S. Dosimetric investigation of lung tumor motion compensation with a robotic respiratory tracking system: an experimental study. Med Phys. 2008;35(4):1232–40.
16. Chan MK, Kwong DL, Ng SC, Tong AS, Tam EK. Accuracy and sensitivity of four-dimensional dose calculation to systematic motion variability in stereotactic body radiotherapy (SBRT) for lung cancer. J Appl Clin Med Phys. 2012;13(6):3992.
17. Inoue M, Shiomi H, Iwata H, et al. Development of system using beam's eye view images to measure respiratory motion tracking errors in image-guided robotic radiosurgery system. J Appl Clin Med Phys. 2015;16(1):100–11.
18. Sumida I, Shiomi H, Higashinaka N, Murashima Y, Miyamoto Y, Yamazaki H, Mabuchi N, Tsuda E, Ogawa K. Evaluation of tracking accuracy of the CyberKnife system using a webcam and printed calibrated grid. J Appl Clin Med Phys. 2016 Mar 8;17(2):74–84.
19. Akino Y, Sumida I, Shiomi H, Higashinaka N, Murashima Y, Hayashida M, Mabuchi N, Ogawa K. Evaluation of the accuracy of the CyberKnife Synchrony Respiratory™ Tracking System using a plastic scintillator. Med Phys. 2018. https://doi.org/10.1002/mp.13028.
20. Cheung K, Lam W, Geng H, Wong R, Ho R, Kong C, Wu P, Yu S. MO-F213AB-05: commissioning of gated RapidArc radiotherapy for treatment of moving targets. Med Phys. 2012;39:3872.
21. Kilby W, Dooley JR, Kuduvalli G, Sayeh S, Maurer CR Jr. The CyberKnife Robotic Radiosurgery System in 2010. Technol Cancer Res Treat. 2010;9(5):433–52.
22. Jung J, Song SY, Yoon SM, et al. Verification of accuracy of CyberKnife tumor-tracking radiation therapy using patient-specific lung phantoms. Int J Radiat Oncol Biol Phys. 2015;92:745–53.
23. Nakayama M, Nishimura H, Mayahara H, Nakamura M, Uehara K, Tsudou S, Harada A, Akasaka H, Sasaki R. Clinical log data analysis for assessing the accuracy of the CyberKnife fiducial-free lung tumor tracking system. Pract Radiat Oncol. 2018;8(2):e63–70.
24. Yang B, Geng H, Ding Y, Kong CW, Cheung CW, Chiu TL, Lam WW, Cheung KY, Yu SK. Development of a novel methodology for QA of respiratory gated and VMAT beam delivery using Octavius 4D phantom. Med Dosim. 2018. https://doi.org/10.1016/j.meddos.2018.02.008.